Carrier-carrier and carrier-phonon interactions in the dynamics of photoexcited electrons in graphene

2015 J. Phys.: Conf. Ser. 647 012003

(http://iopscience.iop.org/1742-6596/647/1/012003)

Journal of Physics: Conference Series **647** (2015) 012003 doi:10.1088/1742-6596/647/1/012003

Carrier-carrier and carrier-phonon interactions in the dynamics of photoexcited electrons in graphene

J. M. Iglesias, M. J. Martín, E. Pascual and R. Rengel

Applied Physics Department, University of Salamanca, Plaza de la Merced, S/N, Salamanca 37008, Spain

E-mail: josem88@usal.es

Abstract. In this work we use the Monte Carlo method to simulate the photoexcited carrier relaxation dynamics in suspended monolayer graphene to unveil the role of the different scattering mechanisms involved. The results show a strong activity of carrier-carrier and carrier-optical phonon interactions in the very early stages of the relaxation process driving the thermalization and cooling dynamics. The consideration of the coupling between the electron and phonon population reveals an intense damping in the cooling rates that is dependent on the pumped carrier concentration.

1. Introduction

Due to its outstanding electronic and optical properties[1] graphene has become a promising material for future developments of a wide range of highly efficient photonic and optoelectronic applications. Its gapless linear band structure makes graphene particularly interesting for novel devices working in the THz spectral range[2, 3]. Experiments comprising pump-probe differential transmission spectroscopy with time resolutions in the femtosecond scale [4–6] provide, from a macroscopic interpretation, insight into the far-of-equilibrium hot carrier dynamics that takes place after photoexcitation. This dynamics can be split in intraband and interband processes. The first consists of a very fast thermalization of the carriers driven by the energy-conserving dual carrier scattering which spreads the electron distribution around the highly populated energy level associated with the wavelength of the optical excitation, leading to a very fast depletion thereof, accompanied with a simultaneous cooling starred by the intrinsic and substrate phonons cascade emissions as the main relaxation mechanisms. Electron-hole recombination completes this carrier dynamics towards the full thermodynamic equilibrium.

Here we will study the intraband thermalization and cooling by means of ensemble Monte Carlo simulations. This methodology allows to tackle the electron dynamics from a particle approach: the system is described by a number of superparticles that resembles a group of electrons (or holes), which are simulated one by one during consecutive time steps, thus allowing the tracking of different quantities, such as the average carrier energy, distribution functions in energy and K-space or the scattering mechanisms undergone per electron. The main features of the model are described in previous works.[7, 8] The contributions of the interactions driving the described processes are the transverse-acoustic (TA), longitudinal-acoustic (LA), transverse-optic (TO), longitudinal-optic (LO) phonon branches. In addition, impurity and imperfection (defects) scattering are included; however, they are disregarded in the present work due to their

single-particle elastic nature. Due to the strong coupling between carriers in graphene, short range carrier-carrier (e-e) scattering is modelled through a static Coulomb screened potential model[9]. The time step in the simulation is set to 0.5 fs. The scattering probabilities are updated every time step. Screening potentials for impurities and electrons are considered by numerically calculating the Lindhard dielectric function in the static limit[10] from the actual energy distribution function obtained in the simulation in order to grant an adequate description of the polarizability under the initial far-from-equilibrium state. The graphene sample is considered to be suspended. Finally, the effect of the hot electron-hot phonon coupling is also incorporated. The population of each phonon mode is updated every time step on a gridded q-space accounting for an histogram of emissions and absorptions and a decay within a relaxation time approximation for lifetimes $\tau_{op} = 2.5$ ps[11] and $\tau_{ac} = 5$ ps[12].

We perform simulations for various pumping energies and concentrations (resulting of different pump fluences), setting an initial carrier distribution according to the expression $f(\varepsilon) = F(\varepsilon, T, \mu = 0) + g_{max} \exp\left[-(\varepsilon - \varepsilon_{photon}/2)^2/2\sigma^2\right]$, where the first member of the RHS is the Fermi equilibrium distribution for intrinsic graphene ($\mu = 0$) and the second represents the excited carriers arising from optical pumping of a light source with an spectral bandwidth peaked at ε_{photon} and σ accounting for a gaussian Fourier bandwidth limited pulse. Possible puddle states were not considered. The parameter g_{max} is the maximum occupation at $\varepsilon = \frac{1}{2}\varepsilon_{photon}$ and relates the pumped concentration with the radiation fluence and the pulse bandwidth.

2. Results

In the first place, we examine the time evolution of the energy distribution function in a generic case to discern the role of the interactions involving the mentioned relaxation dynamics. Figure 1-a shows the evolution of the carrier energy distribution function vs. time, when only e-e interactions are activated, and phonon scattering is disregarded. The results stand out the fast depletion of the electron population at the pumped energy level, since at $t = 100$ fs there is no trace of the initial gaussian distribution. Under these circumstances, carriers spread around the pumped energy level until reaching a thermal distribution at approximately $t = 250$ fs. Let us now check this evolution if e-e interactions are turned off and phonon scattering is activated (fig. 1-b). Cascade phonon emission is clearly visible as the initial pumped gaussian population peak replicates itself at lower energies with a separation corresponding to the energy of the intrinsic optical phonon (165 meV). Finally, fig. 1-c illustrates the dynamics with the full

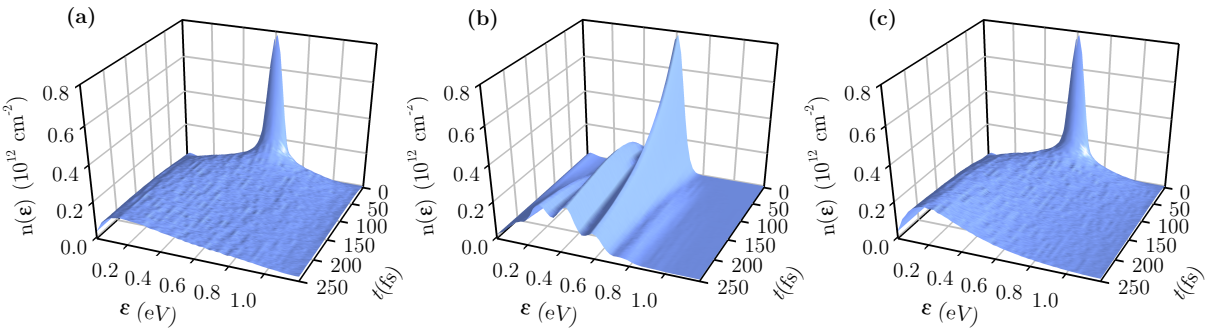

Figure 1. Energy distribution function vs. time obtained from Monte Carlo simulations of (a) the carrier thermalization (phonon scattering turned off), (b) carrier cooling (electron-electron interaccions turned off) and (c) full carrier dynamics during the first 250 fs. Photon energy is $\hbar\omega = 1.2$ eV and $n_s = 5 \times 10^{12}$ cm^{-2}.

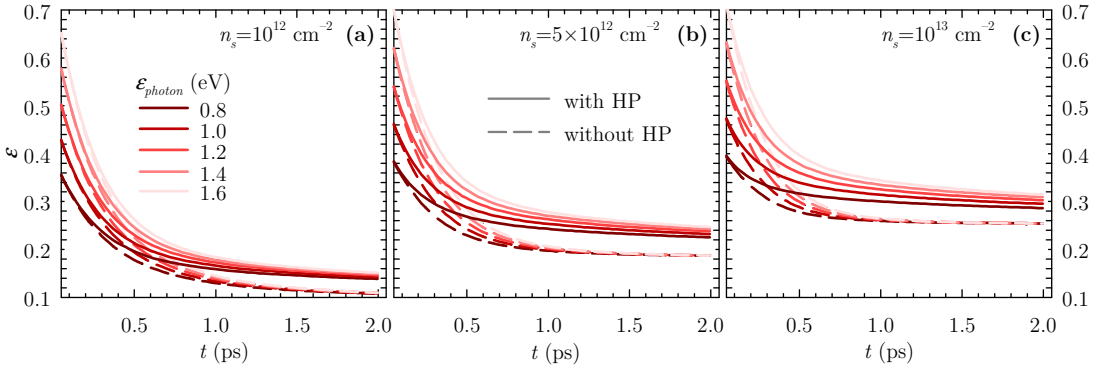

Figure 2. Time evolution of the average system energy considering equilibrium and hot phonon (HP) populations as a function of the pumped carrier density for excited concentrations (a) 10^{12} cm^{-2}, (b) 5×10^{12} cm^{-2}, and (c) 10^{13} cm^{-2}

intraband interactions, where e-e scattering and inelastic phonons interplay between each other: the depletion rate at the excitation energy obeys that of the "e-e only" case, while carriers tend to occupy lower energy levels as time passes as a result of phonon emission. A correct description of hot carrier dynamics involves the consideration of the coupling between charge carriers and the interacting phonons. In particular, hot electrons are expected to emit phonons that, in turn would be out of equilibrium (hot) as well. As a result, the cooling of the carriers is related to that of the phonons, which end up reaching a population distribution according to the lattice temperature thereof. To examine this effect, we have analysed a situation where the phonon population is considered to be in equilibrium and another case for which a hot phonon population (coupled to phonon emission and absorption by carriers) is taken into account. Fig. 2 shows the average system energy, $\varepsilon(t) = \sum_0^N \varepsilon_i(t)/N$ where $\varepsilon_i(t)$ is the energy of each superparticle at a given time and N is the total number of superparticles. In the first place, we observe that the decrease of the system energy is biexponential. Without considering the coupling between carrier and phonon population, all the curves for given n_s tend to overlap. For the lowest electron density ($n_s = 10^{12}$ cm^{-2}) the average energy continues decaying at 2.0 ps but for $n_s = 5 \times 10^{12}$ and $n_s = 10^{13}$ cm^{-2} the average energy reaches its minimum at around 1.8 and 1.4 ps respectively. When hot phonons are included in the dynamics, the initial decay rate is less pronounced as phonon emission instantaneously stimulates its re absorption, pushing carriers back towards higher energies and slowing down the process. Also, the later section of the curves show higher values and the average energies for different pumping wavelengths do not overlap for this time scale showed in the figure, remaining at higher values those of carriers excited with shorter wavelengths. This discrepancy between the hot-phonon and phonon at equilibrium cases is more evident with higher electron density.

One of the most relevant quantities provided by the Monte Carlo method is the scattering count over time, which sheds light on the role of each interaction driving carrier relaxation dynamics. In the fig. 3 we show the time evolution of the average number of intrinsic phonon and e-e scatterings per unit time undergone by a single carrier as a function of the pumping energy. For both scattering mechanisms the initial activity grows linearly with the pumping energy; however the rate of e-e scatterings is one order of magnitude higher. In all cases, e-e interaction drops faster in the first picosecond due to the reduction of the coupling of the excited population; the trend for both intrinsic phonon and e-e scattering is to increase with the photon energy, being this phenomenon more evident at increasing carrier densities. In the latest 500 fs of the sampled time, the scattering rates tend to become independent of the pumping energy,

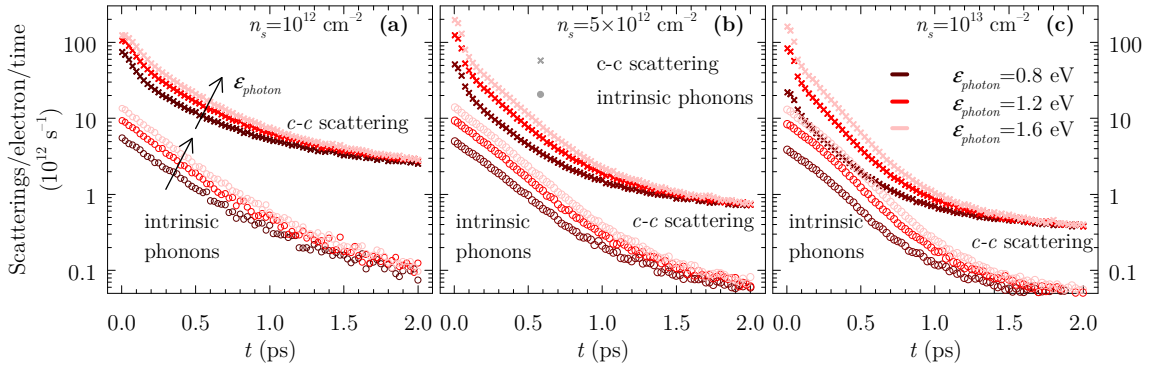

Figure 3. Time evolution of the average number of scatterings per unit time as a function of the pumping energy for (a) $n_s = 10^{12}$ cm^{-2} (b) $n_s = 5 \times 10^{12}$ cm^{-2} and (c) $n_s = 10^{13}$ cm^{-2}

since the system tends to the same quasy-equilibrium distribution functions. In this last section of the plot the carriers with more scattering activity correspond to the situations where the quasi-Fermi surface is smaller (reduced stimulated carrier concentrations).

3. Conclusions

We present a Monte Carlo model for the study of the early stages of the ultrafast intraband relaxation dynamics in monolayer graphene. The role of the most relevant scattering mechanisms (intrinsic phonons and e-e coulomb interactions) ruling this dynamics are disentangled along the time under investigation. The results show that high-energy electron stimulated heated phonon population results in a lower cooling rate of the carriers. Carrier-carrier scattering is the most active interaction and exhibits the fastest drop in the first tens of femtoseconds as a consequence of the depletion of the excited energy levels.

Acknowledgments

This work was supported by research project TEC2013-42622-R from the Ministerio de Economía y Competitividad.

References

[1] Novoselov K S, Geim A K, Morozov S V, Jiang D, Katsnelson M I, Grigorieva I V, Dubonos S V and Firsov A A 2005 *Nature* **438** 197–200
[2] Sensale-Rodriguez B, Yan R, Kelly M M, Fang T, Tahy K, Hwang W S, Jena D, Liu L and Xing H G 2012 *Nat Comms* **3** 780
[3] Ryzhii V, Dubinov A A, Otsuji T, Mitin V and Shur M S 2010 *J. Appl. Phys.* **107** 054505
[4] Sun D, Divin C, Mihnev M, Winzer T, Malic E, Knorr A, Sipe J E, Berger C, de Heer W A, First P N and Norris T B 2012 *New Journal of Physics* **14** 105012
[5] Winnerl S, Göttfert F, Mittendorff M, Schneider H, Helm M, Winzer T, Malic E, Knorr A, Orlita M, Potemski M, Sprinkle M, Berger C and de Heer W A 2013 *Journal of Physics: Condensed Matter* **25** 054202
[6] Tielrooij K J, Song J C W, Jensen S A, Centeno A, Pesquera A, Zurutuza Elorza A, Bonn M, Levitov L S and Koppens F H L 2013 *Nat Phys* **9** 248–252 ISSN 1745-2481
[7] Rengel R and Martín M J 2013 *J. Appl. Phys.* **114** 143702
[8] Rengel R, Pascual E and Maríin M J 2014 *Applied Physics Letters* **104** 233107
[9] Li X, Barry E A, Zavada J M, Nardelli M B and Kim K W 2010 *Applied Physics Letters* **97** 082101
[10] Hwang E H and Sarma S D 2007 *Physical Review B* **75**
[11] Wang H, Strait J H, George P A, Shivaraman S, Shields V B, Chandrashekhar M, Hwang J, Rana F, Spencer M G, Ruiz-Vargas C S and et al 2010 *Appl. Phys. Lett.* **96** 081917 ISSN 0003-6951
[12] Bonini N, Garg J and Marzari N 2012 *Nano Letters* **12** 2673–2678